Proceedings of the 2nd International Conference on Modern Medicine and Global Health
DOI: 10.54254/2753-8818/15/20240482

Investigation of the mechanism of huangqi and danggui decoction in treating non-small-cell lung cancer based on network pharmacology

Xinyu Chang[1, 2, 3, †], Xinyun Zhang[1, 4, †], Zijian She[1, 5, †]

[1]YK Pao School, Shanghai, China
[2]Corresponding author

[3]s19514@ykpaoschool.cn
[4]sophiezhang2703@gmail.com
[5]Szjpeter@163.com
[†]These authors contributed equally to this work and should be considered co-first authors.

Abstract. Non-small-cell lung cancer (NSCLC) accounts for approximately 80% of lung cancer cases, which is a leading cause of cancer mortality worldwide. While therapies such as chemotherapy, radiation, immunotherapy and targeted drugs have shown efficacy, resistance remains a major obstacle. Traditional Chinese medicine (TCM) offers a multi-target approach that may help overcome resistance. This study analyzed the active ingredients of Huangqi and Danggui decoction (HQDGD), a classic TCM formula, and their effects on NSCLC using network pharmacology and experimental validation. Active compounds were identified from TCM databases and linked to gene targets using prediction tools and were compared to NSCLC-related genes to find shared targets. Protein-protein interaction network analysis and pathway enrichment analysis were used to find HQDGD's pharmacology and experiments on lung cancer A549 cells validated that key HQDGD compounds curcumin, quercetin and α-angelicalactone inhibited proliferation and migration, suppressed JAK2/STAT3 activation, and downregulated downstream HIF1A and VEGF. The multi-target actions of HQDGD may overcome resistance in NSCLC. Our integrated computational and experimental approach elucidated the compound-target-pathway mechanisms of a TCM formula against NSCLC, supporting future drug development and research.

Keywords: Huangqi And Danggui Decoction, Non-Small-Cell Lung Cancer (NSCLC), IL6-JAK-STAT3 Pathway, Curcumin, Quercetin And Alpha-Angelica Lactone.

1. Introduction

Lung cancer is the second leading cause of global cancer mortality, accounting for an estimated 2.8 million deaths worldwide annually [1]. Non-small-cell lung cancer (NSCLC) is the major histological subtype of lung cancer, comprising nearly 80% of all cases [2]. Conventional treatments for NSCLC are based on radiotherapy or chemotherapy; however, these treatments are often associated with low prognosis and a significant reduction in life quality [3]. More effective treatments for NSCLC include

DOI: 10.54254/2753-8818/15/20240482

targeted drug therapy and immunotherapy, which are constituted of immune-checkpoint inhibitors and kinase inhibitors for oncogenic driver mutations [2, 4].

Although certain targeted and immuno-therapy strategies have expressed high efficacy in clinical use, with drugs such as gefitinib and afatinib having response rates of 50-80%, the five-year survival rate of NSCLC remains as low as 4-17% [5]. Moreover, widespread drug resistance has rendered these treatments either incomplete or temporary. General resistance mechanisms to targeted agents can be classified intrinsic resistance, in which patients harbor driver oncogenes insensitive to therapy; adaptive resistance, in which tumor cells undergo adaptations that allows their survival after therapy; and acquired resistance, which is a combination of the previous two mechanisms [2, 6]. Hence, new treatment strategies for NHSCLC are urgently required.

In recent years, traditional Chinese medicine (TCM) has been gaining increasing attention due to its reduced toxicity to patients, fewer side effects, and significant synergistic effects when used in combination with Western medication [7, 8]. Contrary to the "one disease, one drug" paradigm of modern pharmaceutics, TCM employs a "multi-component, multi-target, and multi-pathway" approach. The basic hallmark of TCM is the utilization of formulae, where multiple botanical drugs are combined based on compatibility theories to increase treatment efficiencies. This provides an alternative approach to resolving drug safety, as new agents aren't strictly required for the creation of new formulae and therapeutic strategies [8-10].

Huang-qi Dang-gui decoction (HQDBD) is a representative TCM formula which consists of herbal ingredients Dang-Gui and Huang-Qi in a 5:1 ratio [11]. Dang-Gui, or *Angelica Sinensis Radix* (ASR), is the dried roots of *Angelica sinensis*, while Huang-Qi, or *Astragali Radix* (AR), is the dried roots of *Astragalus membranaceus* [11-13]. DBD is famous for its immune regulatory effects and hematopoietic functions. Previous studies have shown that HQDBD demonstrates significant enhancement in the tumor growth inhibition effects when used in combination with targeted drugs such as gemcitabine in NSCLC [14-16]. However, the complex chemical components of HQDBD and its unknown interactions with the human body make it difficult to derive the molecular mechanism, further limiting its development and clinical usage [14, 15].

The establishment of TCM databases such as TCMID and TCMSP has brought forth network pharmacology as a novel approach to predict and analyze the molecular targets of herbs in DBD. Network pharmacology is an emerging technology of drug research and design that utilizes bioinformatic tools to screen complex protein/gene interactions for potential drug targets [17, 18].

In our work, we extracted the active ingredients of HQDBD from several different databases and predicted their targets using Swiss Target Prediction. Related genes of NSCLC were obtained using DisGeNET and GeneCards. We then screened the common genes of NSCLC targets and DBD targets, constructed a protein-protein-interaction (PPI) network, and analyzed the genes' functions in biological processes (BPs), cell components (CCs), and molecular functions (MFs). Finally, we verified the predicted genes and pathway by treating the active ingredients with A549 cells, which is a cell line derived with from carcinogenic pulmonary epithelial cells that's commonly used to model NSCLC. We conducted several assays to validate the inhibitory efficacy of different treatment combinations on the cell proliferation, cell migration, and apoptosis of A549 cells. Our experimentation also revealed insights on the cell signaling pathways and corresponding genes downregulated by HQDBD ingredients.

2. Materials and Methods

2.1. Network pharmacology-based analysis

2.1.1. Active Ingredients in HQDGD. The list of chemical ingredients in Huangqi and Danggui were first obtained from HERB, a comprehensive Traditional Chinese medicine database that sites information from Pubmed, TCMID and other databases [19]. Since Huangqi and Danggui decoction are prescribed for oral administration, ingredients were assessed for Oral bioavailability (OB) and Drug-likeliness (DL). The selection criteria was OB $\geq$ 30% and DL $\geq$ 0.18. However, ingredients that don't

DOI: 10.54254/2753-8818/15/20240482

have experimental OB and DL values were predicted using Swiss ADME target prediction tool, which evaluates the drug-likeliness of ingredients according to their SMILES [20]. For such ingredients, the selection criteria were less than two violations of the Lipiski (Pfiezer) filter, which is Mw ≤ 500, ALogP ≤ 5, Hdon ≤ 5 and Hacc ≤ 10.

2.1.2. Gene Targets Related to Active Ingredients. The related gene targets of the selected bioactive ingredients in HQDGD were collected using Swiss Target Prediction [21], a tool available online. Using the ingredients' obtained smiles as input and selecting "Homo sapiens" as the species, the algorithm compares the ingredient to its set of 370,000 experimentally molecular interactions in Release 15 of the ChEMBL database [22] and makes protein targets prodiction according to the "similarity principle", which states that two similar molecules are prone to have similar properties. Covering most of the main "druggable targets", we then only kept targets for each ingredient that has probability of higher than 5%. At last, we used the genes' common name in UniProt [23] in all scenarios.

2.1.3. Known Targets of NSCLC. Related genes to non-small-cell lung cancer were obtained from gene cards [24] and disgenet [25], using "non-small-cell-lung-cancer" as the keyword. In GeneCards,920 protein coding genes are kept. In Disgenet, 12, 13, 11 and 11 related genes are found for NSCLC Recurrent, Stage IIIB, Stage IIIS and Stage II, and all are kept. The genes appearing multiple times are sieved and the result was standarized using their common name.

2.1.4. Shared Gene Targets for HQDGD and NSCLC. Using the sieved gene targets for both HQDGD ingredients and NSCLC genes, the common targets for the two categories were visualised using a venn diagram. The venn diagram is constructed using jvenn, an online graph construction tool [26]. Each gene target's common name was used for comparison in jvenn.

2.1.5. PPI Network Construction. For the construction of protein-protin-interaction (PPI) network disease-ingredient common genes are then imported into String, a database that is able to visually link two proteins that has known and predicted protein–protein interactions. It currently contains approximately 24.6 million proteins from 5,090 organisms [27]. In this investigation, "Homo sapiens" is selected as the organism in search settings.The minimum required interaction score is set at high confidence (≥ 0.7). And, active interaction sources from textmining, experiments, databases, co-expression, heighborhood, gene fusion and co-occurance are all included. The PPI network is visualised in Cytoscape (version 3.10.0) [28] and the betweenness, represented by the size of each node, is analysed using CytoNCA [29], a plugin in Cytoscope.

2.1.6. Network visualization. The disease-ingredients-common targets network was constructed and visualized in Cytoscape (version 3.10.0). Again, CytoNCA app is used to analyze the betweenness of each node, which is visualized by node-size on the network.

2.1.7. GO and KEGG Pathway Enrichment Analysis. The common genes' functions in biological processes (BPs), cell components (CCs), and molecular functions (MFs) is then analysed and described using Gene Ontology (GO) annotation [30, 31]. Further information about genome, chemistry, and system function information is gathered from The Kyoto Encyclopedia of Genes and Genomes (KEGG) database [32-34]. In this study, we've used DAVID Bioinformatics [35], a database that integrated GO and KEGG pathway enrichment analysis. Inputting the common gene, selecting Homo sapien as species and "Gene list" as list type, we exported the Goterms for CCs, MFs and BPs, as well as the relevant KEGG pathways. To obtain more accurate results, we screened for terms with $p < 0.01$. Finally, our Heatmap was plotted by https://www.bioinformatics.com.cn (last accessed on 10 Aug 2023), an online platform for data analysis and visualization.

DOI: 10.54254/2753-8818/15/20240482

2.2. Experimental validation

2.2.1. Preparation of Ingredients. The compounds quercetin (HBIN041495) and curcumin (HBIN021985) were obtained in powder form from Bidepharmatech. α-angelica lactone (HBIN015380) was obtained from Maclin Pharmaceuticals. Quercetin (CAS 117-39-5) and curcumin (CAS 458-37-7) were each purchased in 50 g quantities. α-angelica lactone (CAS 591-12-8) was purchased in two 25 g units. Human IL-6 protein was acquired from MedChemExpress (catalog number HY-P7044) in 10 μg quantities.

2.2.2. Cell culture and treatment. Lung cancer cell lines for A549 were purchased from the cell bank of Shanghai Institute of Biochemistry and Cell Biology. The culture medium was dulbeco-modified eagle culture medium supplemented with 10% fetal bovine serum. The cells are maintained in a humidified incubator at 37°C with 5% CO2 to provide optimal growth conditions.

2.2.3. Cell counting Kit-8 (CCK-8) assay. A549 cells were inoculated into 96-well plates at a density of 0.5 × 104 cells/well. Different concentrations (0, 1, 0.1, 0.01, 0.001, 0.0001, 0.00001 mM) of quercetin (HBIN041495), curcumin (HBIN021985), and alpha-angelica lactone (HBIN016086) were added to the cells. Testing for each concentration was replicated three times. After 24 hours of treatment, cell toxicity was assessed using the CCK-8 Cell Counting Kit from Vazyme and absorbance of each well at 450 nm. Plotting the dose response curve, the 50% (IC50) concentration of the three drugs inhibiting cell growth is obtained.

2.2.4. Investigation of the ingredients' phenotypic effects on NSCLC cells. For investigating of the phenotypic effects of quercetin (HBIN041495), curcumin (HBIN021985), and alpha-angelica lactone (HBIN016086), the cell experiment was divided into 6 groups: control group (A), IL-6 (B), IL-6 with quercetin (C), IL-6 with alpha-angelica lactone (D), IL-6 with curcumin (E), IL-6 with quercetin, alpha-angelica lactone and curcumin. The dosage for each ingredient is the IC50 concentration previously obtained, with 0.1 mM for quercetin, 0.038 mM for curcumin, 1 mM for alpha-angelica lactone and 40 ng/ml for IL-6. 4 tests were conducted on these groups. First, cell proliferation was measured at 24, 48, and 72 hours after treatments using CCK-8 assay. Second, cell migration was assessed 24 hours after treatment using a scratch assay. Images were captured at the start of the assay (0 hours) and after 24 hours to calculate the percentage of wound closure. Third, at 4 hours after treatment, RNA was collected from each group and qPCR was performed to measure mRNA expression of HIF1, HIF2, VEGF, and EGFR. At the same time, protein was collected from each group and Western blot was performed to measure HIF1, HIF2, VEGF and EGF protein levels. The methodologies for western blotting and Q-PCR are given in later section.

2.2.5. Investigation of the ingredients' functional mechanisms on NSCLC cells. For investigating the functional mechanisms of quercetin (HBIN041495), curcumin (HBIN021985), and alpha-angelica lactone (HBIN016086), the cell experiment was divided into 8 groups: (A) control group, (B) IL-6, (C) IL-6 with quercetin, (D) IL-6 with quercetin and JAK2 inhibitor (20 μM), (E) IL-6 with alpha-angelica lactone, (F) IL-6 with alpha-angelica lactone and STAT3 inhibitor (2 μM), (g) IL-6 with curcumin, (h) IL-6 with curcumin with PI3K inhibitor (2 μM). The dosage for each ingredient is its IC50 concentration previously obtained. And, the inhibitors for JAK2, STAT3, PI3K were from Afinity and ZSTK474 from MedChemExpress (MCE) respectively.

Again, cell proliferation was measured at 24, 48, and 72 hours after treatments using CCK-8 assay. Cell migration was assessed 24 hours after treatment using a scratch assay. Images were captured at the start of the assay (0 hours) and after 24 hours to calculate the percentage of wound closure. And, RNA was collected from each group and qPCR was performed to measure mRNA expression of *HIF1*, *HIF2*, *VEGF*, and *EGFR*. Finally, protein was collected from each group and Western blot was performed to measure pJAK2, JAK2, pSTAT3, and STAT3 protein levels.

DOI: 10.54254/2753-8818/15/20240482

2.2.6. Western blot. Proteins are extracted using RIPA buffer from Epizyme, China and the procedure followed the instructions of the total protein extraction kit. BCA assay kit is procured from Vazyme and was used to determine the protein concentration of each sample. Total protein was isolated by 12% SDS-PAGE, then transferred to polyvinylidene fluoride (PVDF) membrane, sealed in TBST consisting of 5% BCS for 30 minutes, incubated overnight with primary antibody, and then incubated at 37℃ for 2 hours with secondary antibody. PDVF was developed in exposure solution, and the gray values of each protein were calculated by ImageJ. The image was analyzed by software, and GAPDH was used as internal reference to determine the gray value of protein bands.

2.2.7. Real-time polymerase chain reaction analysis. Total RNA was isolated from lung cancer cells and used to synthesize cDNA using the HiScript II 1st Strand cDNA Synthesis Kitprimer reverse transcription kit from Vazyme. Quantitative polymerase chain reaction was performed using AceQ Universal SYBR qPCR Master Mix from Vzyme. All RT-PCR was performed at least 3 times. All primers were synthesized by General BioL.

2.2.8. Cell migration Scratch Assay. Six-well plates were seeded with 3×10^5 cells per well and cultured overnight. Afterward, different drug treatments were applied according to the experimental requirements for 24 hours. A straight line was marked using a 200 μl pipette tip as a guide, ensuring that the tip was held vertically without tilting. The marked cells were washed twice with PBS to remove any remaining cells, and fresh culture medium was added for continued incubation. After 24 hours, photographs were taken to observe the size of the marked area.

2.2.9. Statistical analysis. All statistical data were analyzed using GraphPad Prism software V10.0. Comparisons between the groups were evaluated by one-way analysis of variance (ANOVA), and differences between the two groups were measured by Dunnett's test. The experimental data were expressed as mean ± SD. Statistical significance was defined as $p < 0.05$.

3. Results

3.1. Network pharmacology-based analysis

3.1.1. Potential Targets of Active Ingredients. The criteria is set at OB ≥ 30% and, when the experimental OB value of the ingredient isn't available, less than two violations of the Lipinski rule. A total of 200 active ingredients from Herb were found, in which 96 were from Danggui and 104 were from Huangqi. Using Swiss Target Prediction, we identified the related genes for both Huangqi and Danggui. To eliminate redundancy caused by genes appearing multiple times in different ingredients, we refined the list and retained 1,137 potential targets of the active ingredients as the final result.

3.1.2. Common Targets–Active Ingredients Network. From Disgenet and GeneCards, 945 NSCLC-related genes targets were collected. By comparing the targets of NSCLC and HQDGD, we found 189 targets shared by the disease and active ingredients (Figure 1).

DOI: 10.54254/2753-8818/15/20240482

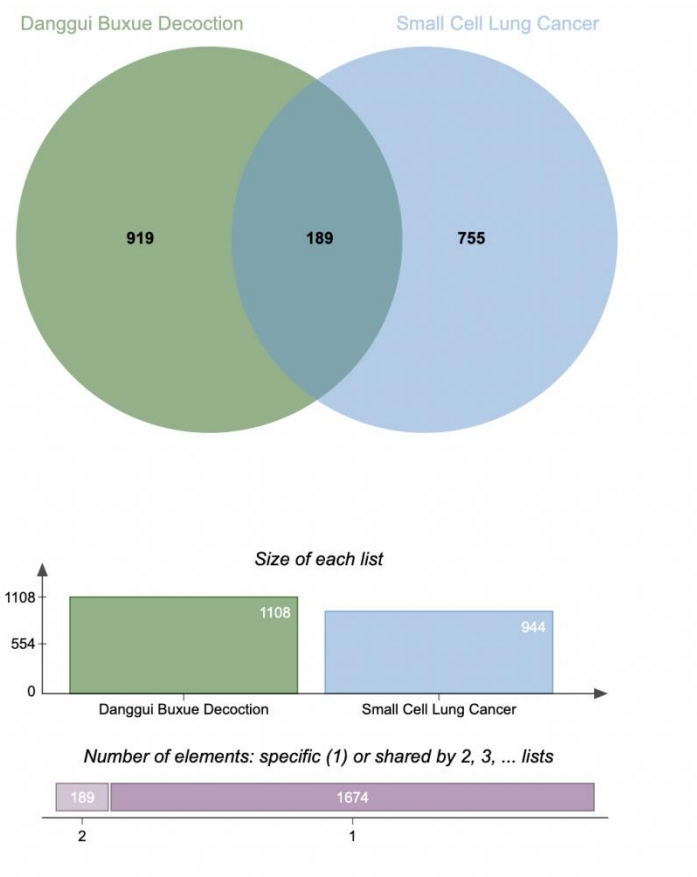

Figure 1. Venn diagram for Common-targets-Active ingredients network. The diagram is constructed using jvenn [26].

The shared target-active ingredients network is shown in Figure 2. We identified 15 key ingredients with degree ≥ 20, namely, senkyunolide E (HBIN043729), kaempferol (HBIN031753), kumugansine A (HBIN031114), (3R)-3-(2-hydroxy-3,4-dimethoxyphenyl)chroman-7-ol (HBIN009497), butanoic acid (HBIN019073), 2-hydroxy-3-methoxystrychnine (HBIN005744), eucalyptin (HBIN026011), 3,5-dimethoxystilbene (HBIN007657), homosenkyunolide (HBIN029511), liensinine (HBIN033162), isoeugenol (HBIN030728), neferine (HBIN036518), linolenic acid (HBIN033339), dihydropinosylvin (HBIN023962), ethyl-p-methoxycinnamate (HBIN025973), isoflavanone (HBIN030736), suchilactone (HBIN045071), Jaranol (HBIN031446), Cnidilin (HBIN021168), nordihydrocapsacine (HBIN037322), curcumin (HBIN021985). Notably, Curcumin has the highest degree (26) and betweenness (996.7) among all ingredients.

DOI: 10.54254/2753-8818/15/20240482

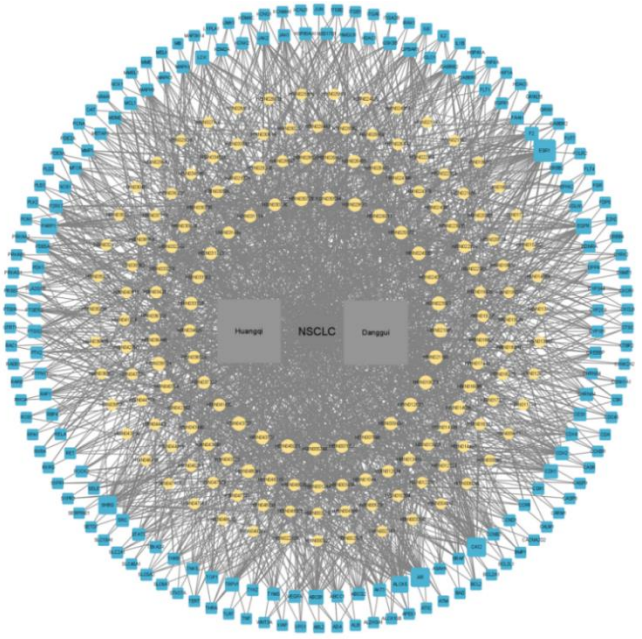

Figure 2. Common targets-active ingredients network. Yellow nodes represent the active ingredients related to the common targets; blue notes represent the common targets. Huangqi and Danggui, the two herbs, and NSCLC, the disease, are placed in the centre of the network. The betweenness of each node is viduaalized by node-size on the network.

3.1.3. PPI Network Analysis of Disease Targets. The protein-protein interaction network analysis on the disease-ingredient shared targets was performed using the String database, as shown in Figure 3. Visualised using Cytoscape, the red nodes in the centre represent the 17 genes with the largest betweeness values, meaning that they are significant in the pharmacology of HQDGD.

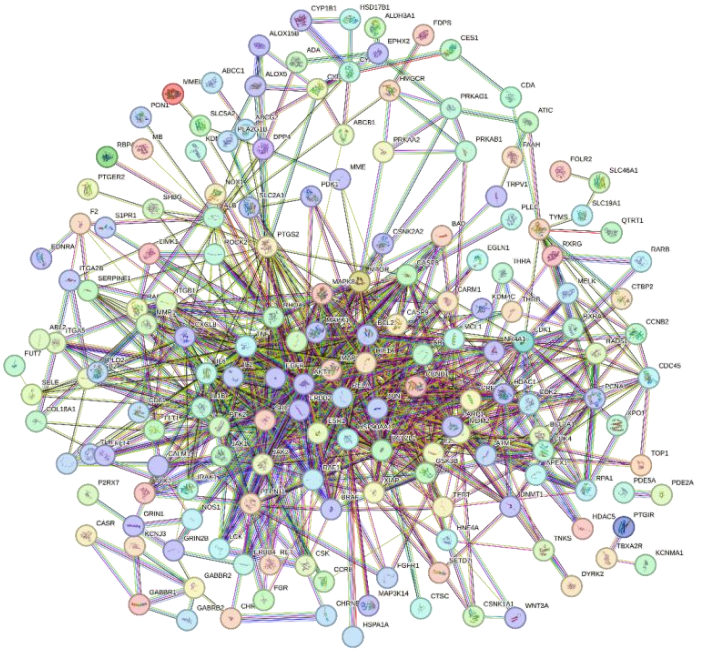

Figure 3. The protein-protein interaction (network) analysis of the shared genes of active ingredients and disease.

DOI: 10.54254/2753-8818/15/20240482

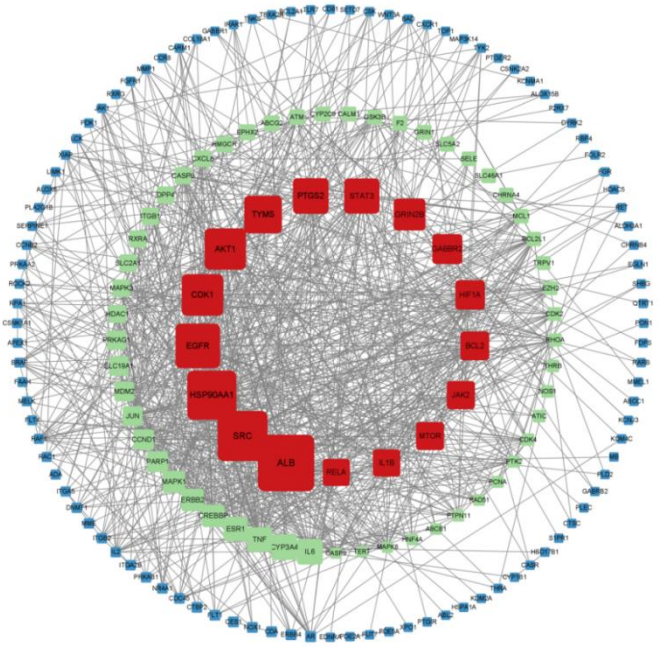

Figure 4. The red nodes in the center represent the 17 genes with the largest betweenness values of 1,100-2,955. The inner green circle contains genes with betweenness 100-1100; the outer blue circle outer has betweenness value 0-100.

3.1.4. Common Targets Enrichment Analysis. The HQDGD and NSCLC common gene targets were analyzed using DAVID Bioinformatics and compared to all known pathways in Homo sapiens [35]. To further screen the result, the top twenty pathways with the lowest p-value were visualized using a heatmap, shown in Figure 5a. The p-value compares how likely the co-occurrence of common gene targets and targets in the pathway is due to chance. A low p-value indicates a high coincidence between the HQDGD and NSCLC common gene targets and targets in the pathway.

To further explore the function of HQDGD ingredients, each gene target common for HQDGD and NSCLC was analyzed using DAVID Bioinformatics for related cellular activities. The summation of their functions was visualized using a heatmap, shown in Figure 5b.

In Figure 5a and 5b, the vertical axis displays the pathways or cellular activities obtained from DAVID bioinformatics. The larger the bulb, the higher, the more HQDGD and NSCLC common gene targets coincide with the indicated pathway/cellular activity. Bulbs with a reddish tint indicate a higher , which suggests a lower p-value and a higher coincidence of HQDGD and NSCLC common gene targets with the pathway/cellular activity.

From Figure 5a, it can be seen that ingredients in HQDGD play a role in lipid and atherosclerosis as well as the P13K-Akt pathway, which is involved in cell proliferation, apoptosis and cell cycle regulation. Figure 5b shows that HQDGD mainly interferes with protein phosphorylation, plasma membrane, nucleoplasm, cytoplasm, cytosol, nuclear functions, and protein binding.

These two graphs provide further information on HQDGD's therapeutic effect, including, but not limited to, treating NSCLC.

DOI: 10.54254/2753-8818/15/20240482

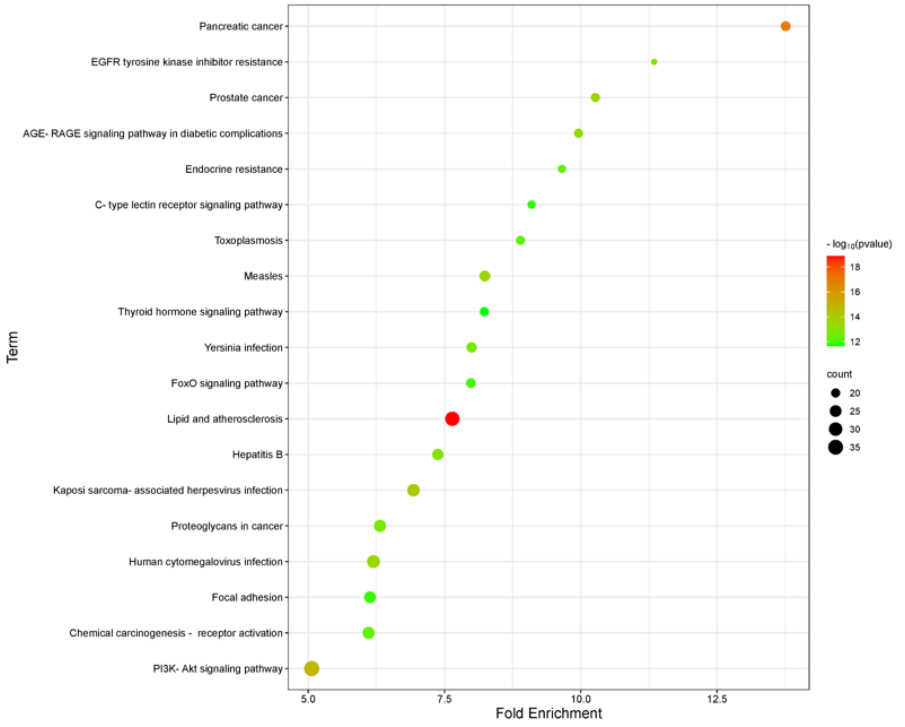

(a)

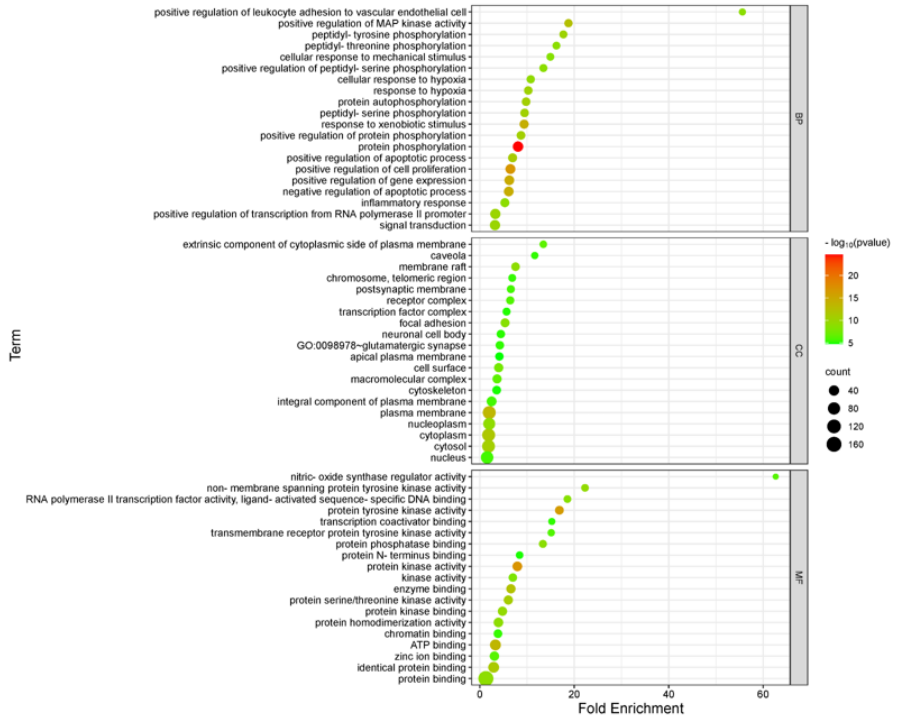

(b)

Figure 5. Heatmap exhibiting the pathways that the top twenty common gene targets with the lowest p-value are involved in. (a) Heatmap comparing the top 20 pathways with the lowest p-value. (b) Heatmap displaying the summation of cellular activities related to HQDGD and NSCLC common gene targets.

DOI: 10.54254/2753-8818/15/20240482

3.1.5. Selecting and Analysing Critical GO and KEGG of HLJDD on NSCLC. Pathways closely related to HQDGD and NSCLC common gene targets were analysed and evaluated in detail using KEGG, an open bioinformatics platform documenting gene targets and corresponding pathways (KEGG). Then, we compared the different pathways and selected ones with a high number of consecutive HQDGD and NSCLC common gene targets for further comparison.

Two pathways were selected preliminarily: Proteoglycans in cancer and Pathways in Cancer.

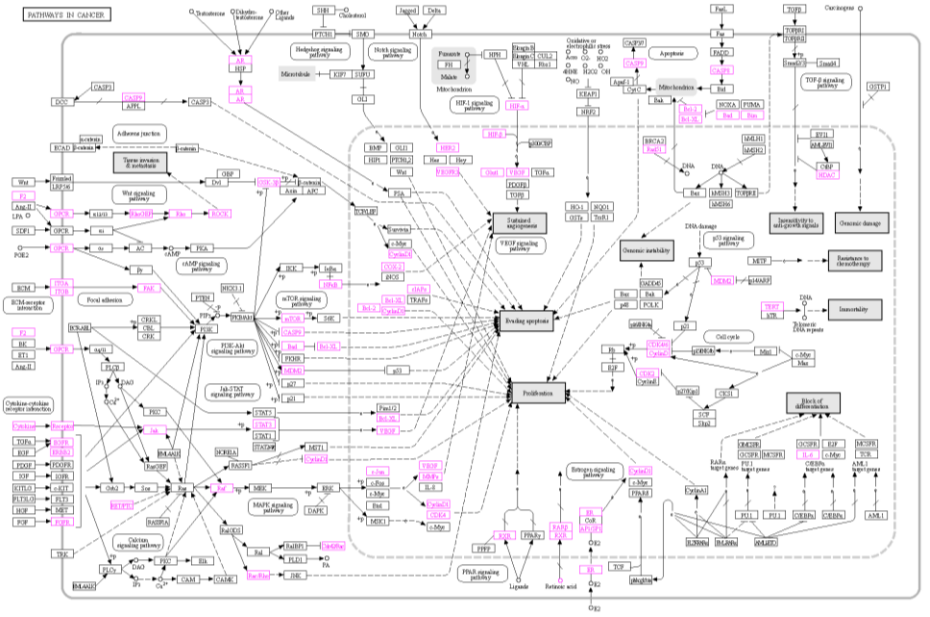

(a)

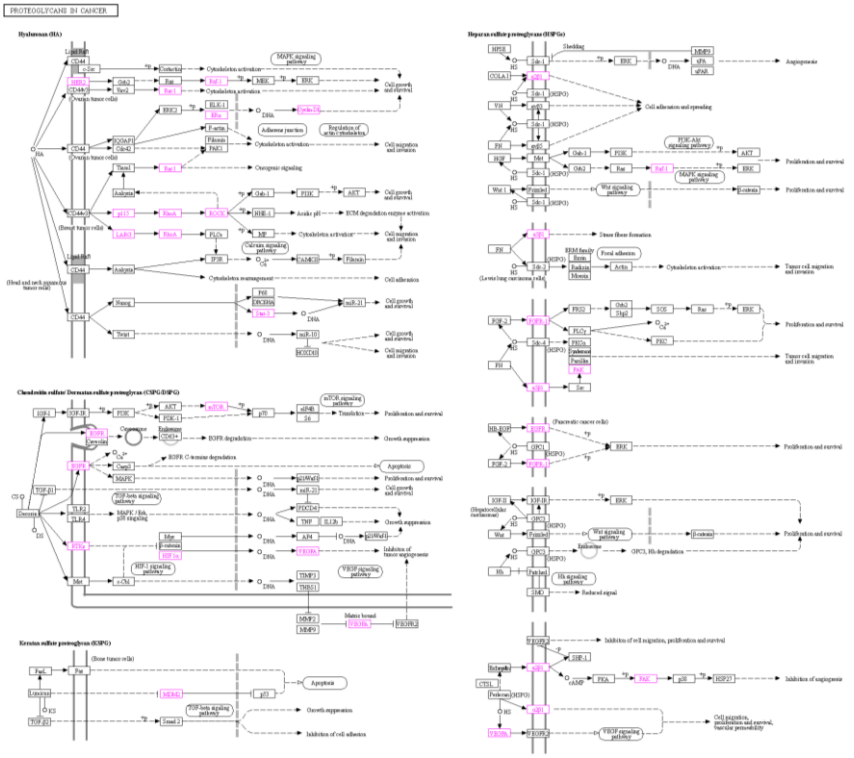

(b)

DOI: 10.54254/2753-8818/15/20240482

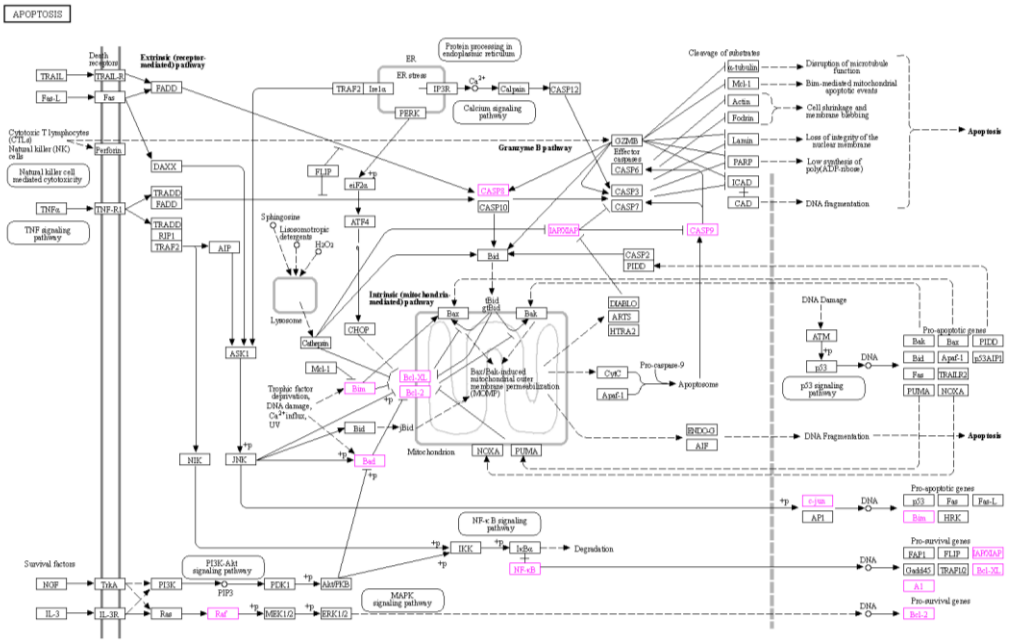

(c)

Figure 6. Pathways with the highest co-occurrence of consecutive HQDGD and NSCLC common gene targets (which are labelled in pink). (a) Pathways in Cancer. (b) Proteoglycans in cancer. (c) Apoptosis.

Individual pathways within the three schematics (Figure 6) were then selected. The selection criterion was equal to or over three consecutive HQDGD and NSCLC common gene targets. Seven pathways fulfil this requirement (Figure 7).

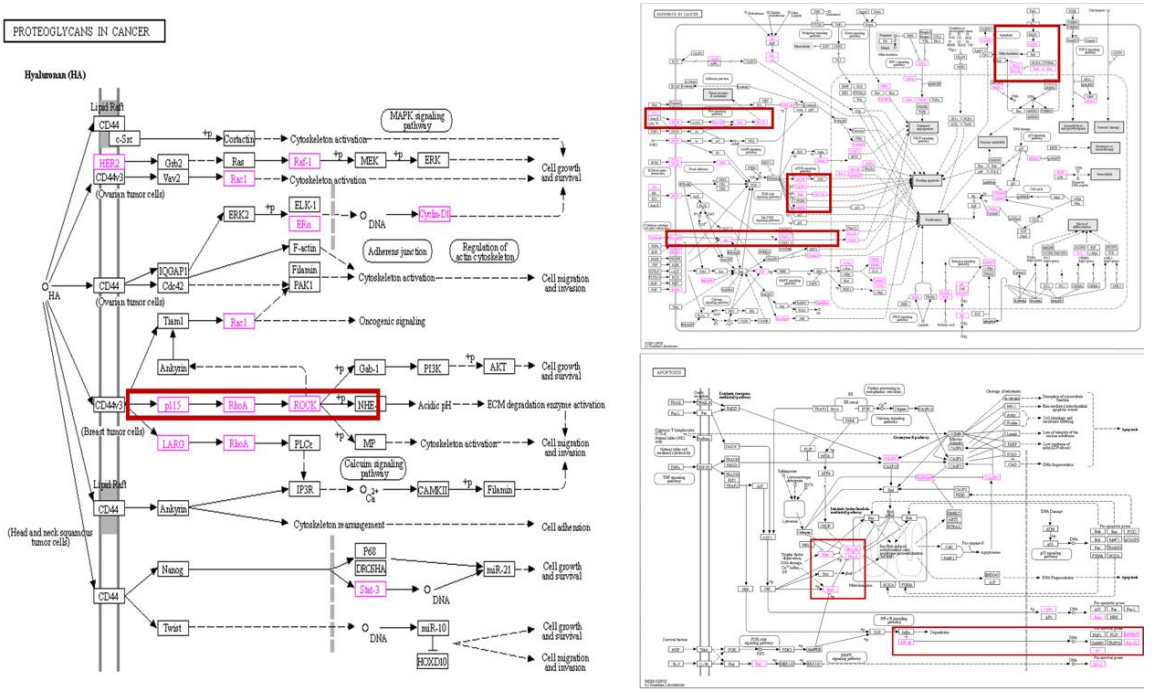

Figure 7. The seven chosen pathways. The selection criteria are set to include three or more consecutive HQDGD and NSCLC common gene targets. The chosen pathways meeting these criteria are indicated using a red box.

DOI: 10.54254/2753-8818/15/20240482

It can be suggested that HQDGD involves in the *p115-RhoA-ROCK*, *F2*-induced signalling pathway, *P13K-Akt* signalling pathway, *Bad* and *Bim* induced mitochondrion suppression pathway, *IL6* (labelled as "Receptor" in Figure 7.) induced *JAK2* and *STAT3* apoptosis evasion pathway, *Bim* and *Bad* induced *Bcl-XL* and *Bcl-2* inhibition, NF-B induced pro-survival gene activation pathway.

Our team collated the HQDGD-NSCLC ingredients corresponding to the gene targets in the pathways mentioned above and further researched the efficacy of these ingredients acting on the gene targets using databases such as Pubmed and Nature. Out of the seven selected pathways, our team conducted experiments testing the efficacy of HQDGD ingredients quercetin, curcumin, and alpha-angelica lactone on interfering with the *IL6-JAK2-STAT3* pathway, as shown in Figure 8. This is because many peer-reviewed articles published on reputable databases have suggested a strong relationship between these ingredients and the selected pathway, and the relationship between individual chemicals and gene targets in the pathway is comparatively more validated than other pathways. Furthermore, upon research, our team found Wang et al.'s study has suggested the *PI3K* that curcumin targets that yield significant anti-proliferative and anti-metastatic properties on NSCLC. Due to the limitation in our gene target prediction procedure, we may have missed this gene target due to the limitation in our method. Hence, our team decided to further investigate the curcumin's suppressive effect on PI3K on top of the aforementioned gene targets.

Therefore, our experiment will examine the effect of quercetin, curcumin and alpha-angelica lactone on the IL6-induced *STAT3/JAK2* pathway, *PI3K*, and NSCLC's proliferative and migrative properties.

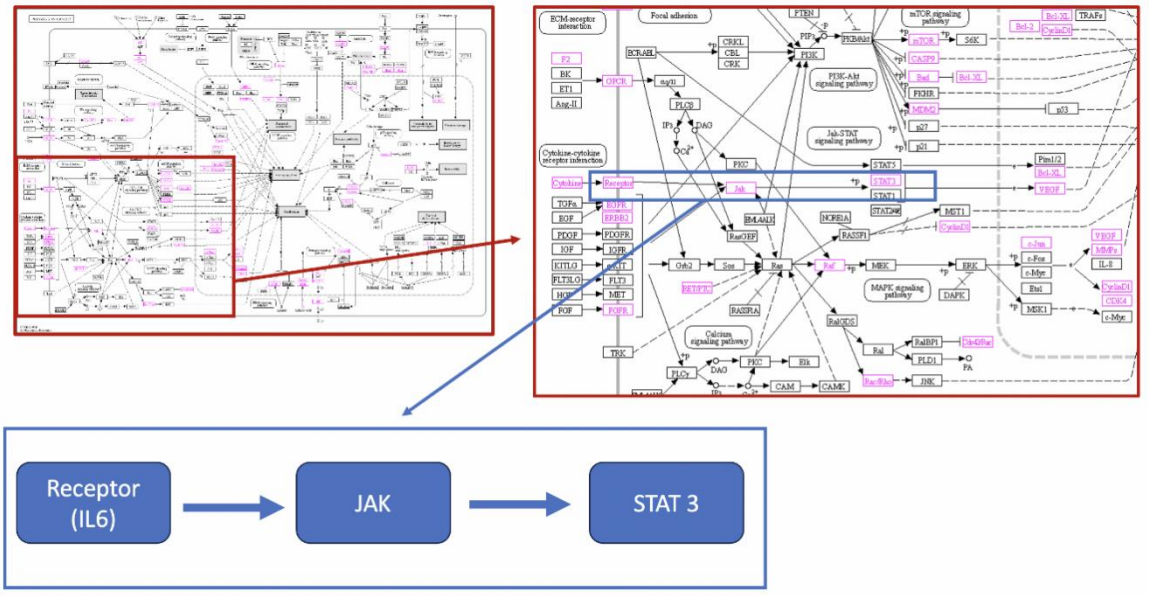

Figure 8. The selected pathway (*IL6-JAK -STAT3*) and target genes.

3.2. Verification by cell experiment

3.2.1. Cytotoxicity of DGBXT. To determine the cytotoxic effects of quercetin, curcumin, and alpha-angelica lactone on lung carcinoma cells, we treated three batches of A549 cells with increasing chemical concentrations for 24 hours each. Corresponding cell viability assays were conducted by the cell-counting kit 8 (CCK-8) and the drug inhibitory effects at each concentration were calculated (shown in Figure 9). The results suggest that the IC50 for quercetin is at a concentration of 0.1 mM, as its inhibitory effects reached 50.56% compared to the control group. The IC50 for curcumin is approximately 0.0379 mM, derived from the fitted IC50 graph (Figure 10). The margin of error is between 0.01 mM and 0.1 mM. For both quercetin and curcumin cell treatments, the inhibitory rates calculated at 1 mM is deemed fallacious. Significant sedimentation occurred at high drug concentrations,

DOI: 10.54254/2753-8818/15/20240482

causing the chemicals to not fully react with the cells and therefore yielding lower inhibitory values. The IC50 of alpha-angelica lactone is also not obtained as the largest concentration (1 mM) only reached 36.18% inhibitory effect. Higher concentrations weren't successfully conjured as impurities and sedimentation rendered the reaction system invalid.

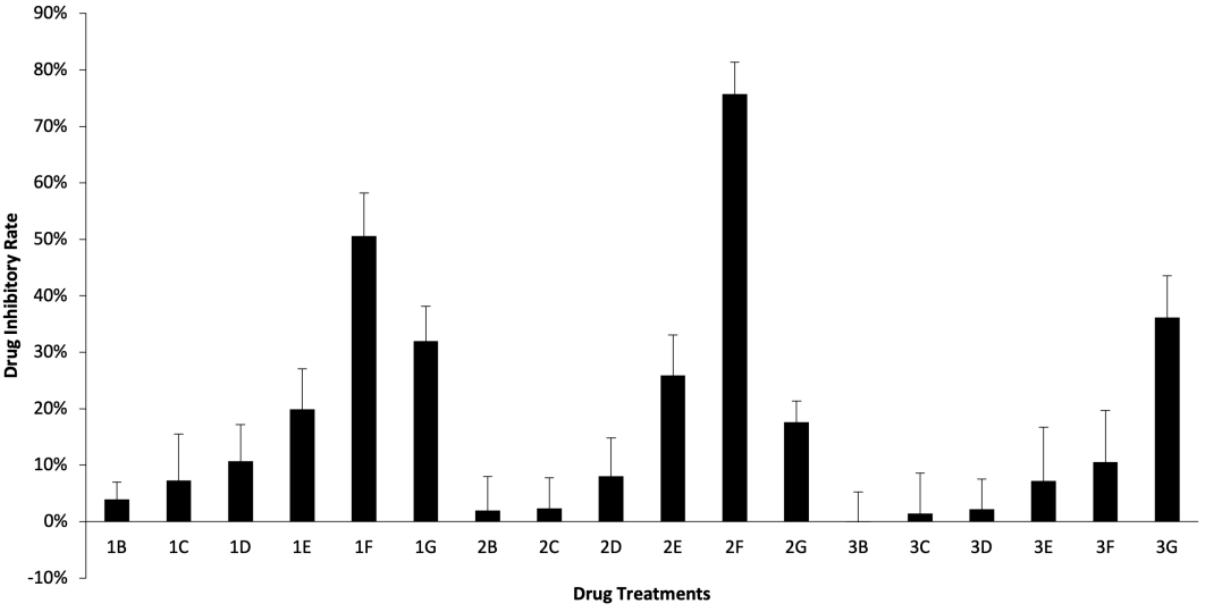

Figure 9. The Inhibitory Rate of IncreasingConcentrations of Quercetin, Curcumin, and Alpha-angelica lactone on A549 Cells. 1B to 1G represents quercetin treatments, 2B to 2G represents curcumin treatments, 3B to 3G represents alpha-angelica lactone treatments. B is 0.00001 mM, C is 0.0001 mM, D is 0.001 mM, E is 0.01 mM, F is 0.1 mM, G is 1 mM.

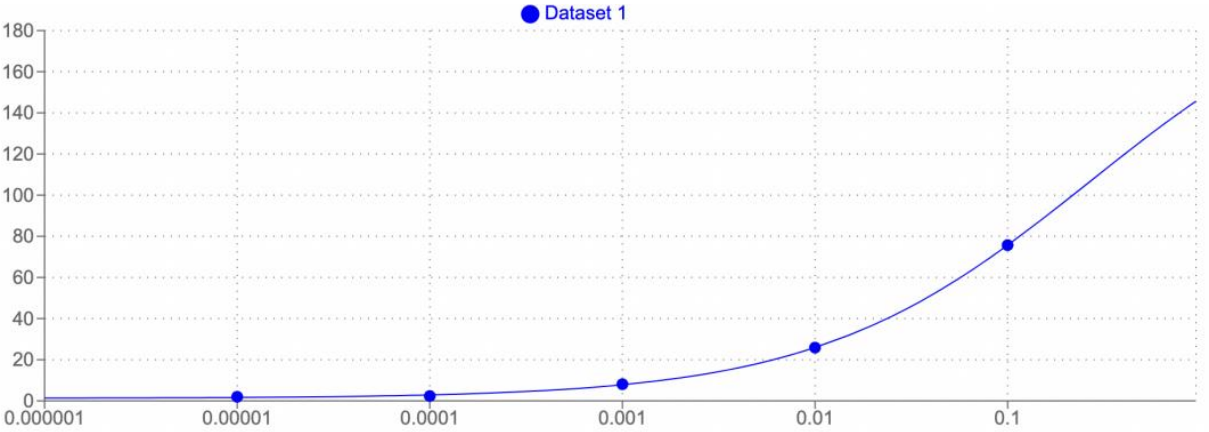

Figure 10. The IC50 Curve for Curcumin Treatment of A549 Cells, fitted with AAT Bioquest.

3.2.2. HQDGD inhibited the activation of the IL-6/JAK/STAT3 signaling pathway of A549 cells. After A549 cell treatments with quercetin, curcumin, alpha-angelica lactone, and interleukin-6 (IL-6), an ingredient of HQDGD, the gene expressions of HIF1, HIF2, VEGF, and EGFR, which are all genes downstream of STAT3, were tested by quantitative polymerase chain reaction (qPCR) analysis. As shown in figure 11, mRNA expression levels for HIF1, HIF2, VEGF, and EGFR decreased in treatments with IL-6 and all three ingredients in comparison to the individual treatments with IL-6. This demonstrates a conspicuous inhibitory effect. Comparatively, alpha-angelica lactone expressed the lowest potency across all four genes. We observed that co-treatments with quercetin, curcumin, and

DOI: 10.54254/2753-8818/15/20240482

alpha-angelica lactone on A549 cells yielded the highest inhibition, suggesting additive effects between the three chemicals.

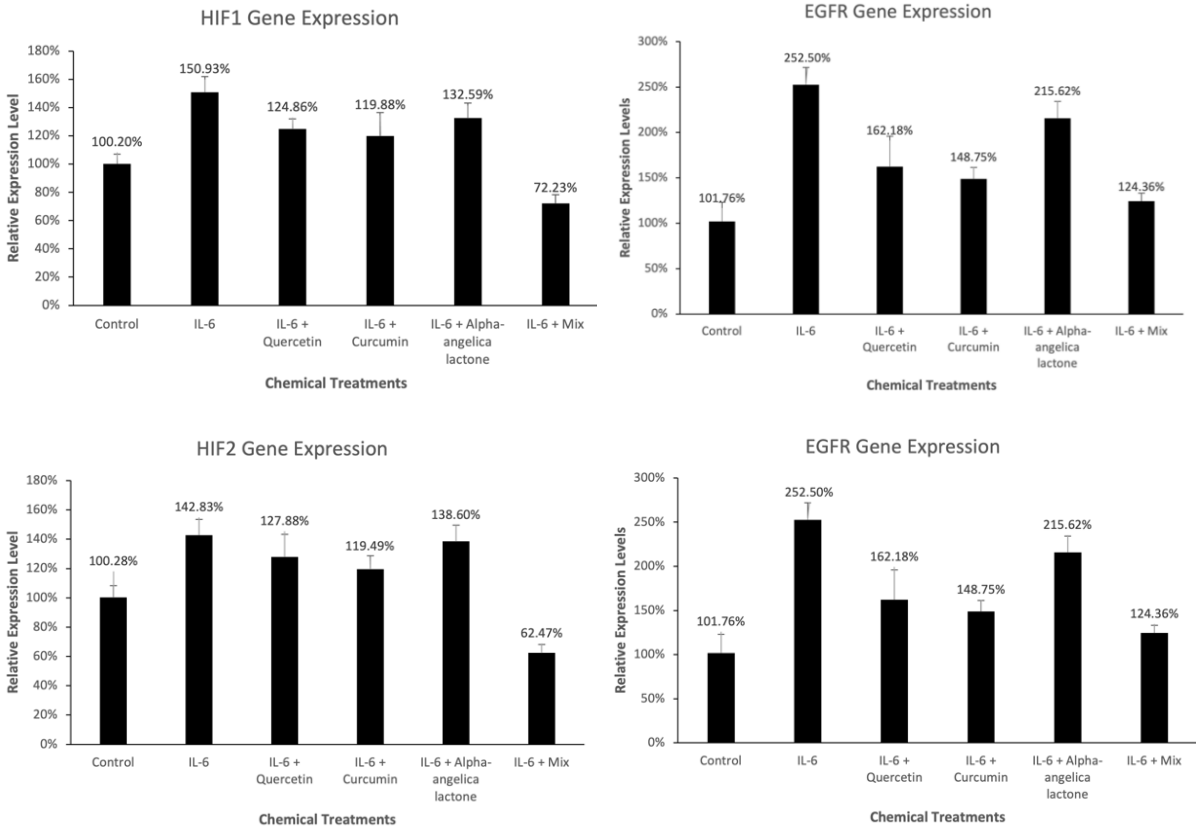

Figure 11. The gene expression levels of the *HIF1*, *HIF2*, *VEGF*, and *EGFR* genes with different combinations of chemical treatments, measured by Q-PCR reaction.

With the further addition of *JAK2* inhibitors to quercetin, *PI3K* inhibitors to curcumin, and *STAT3* inhibitors to alpha-angelica lactone, we observed either similar or lower expression levels of *HIF1*, *HIF2*, *VEGF*, and *EGFR* (shown in Figure 12). This demonstrates that quercetin, curcumin, and alpha-angelica lactone are able to inhibit the activation of *IL-6*, *JAK* and *STAT3* signaling pathway as well as *PI3K* signaling respectively.

DOI: 10.54254/2753-8818/15/20240482

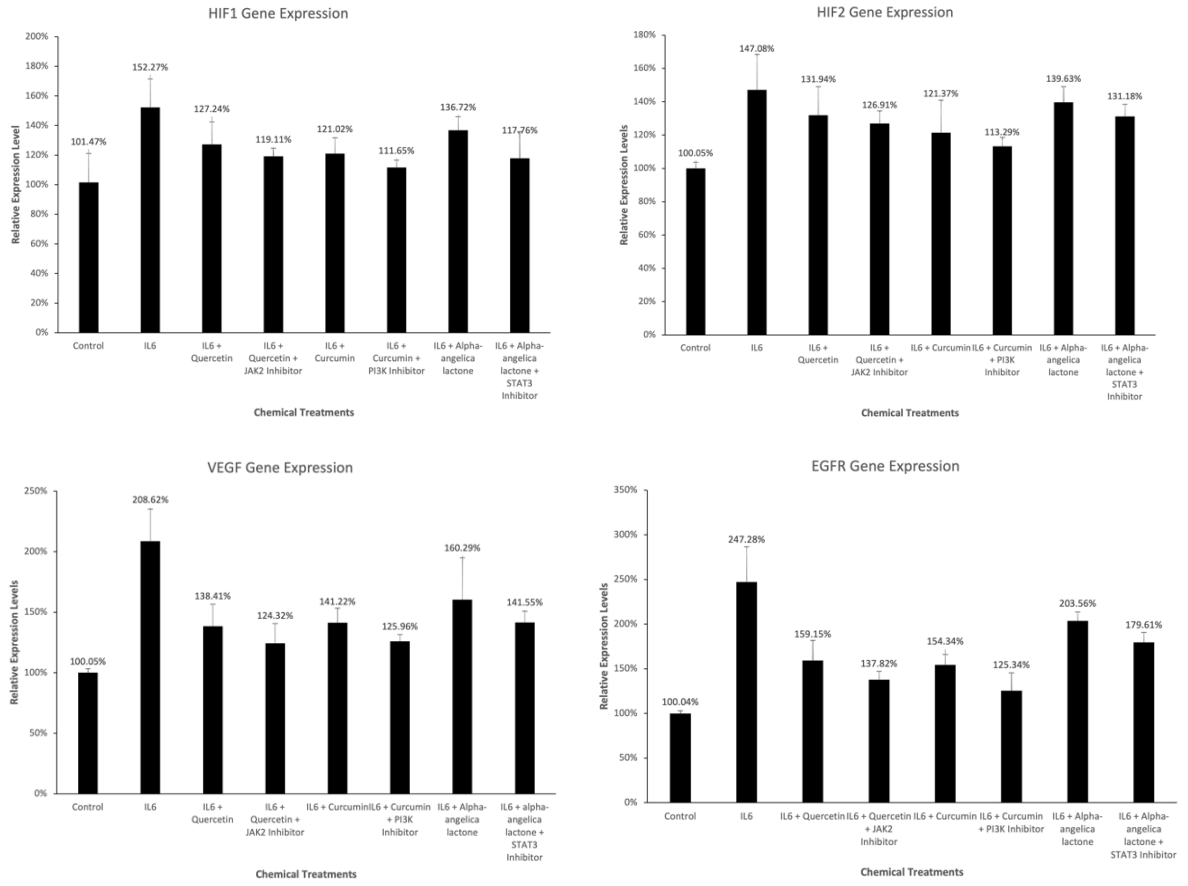

Figure 12. The gene expression levels of the *HIF1*, *HIF2*, *VEGF*, and *EGFR* genes with different combinations of chemical treatments and gene inhibitors, measured by Q-PCR reaction.

3.2.3. HQDGD promotes the apoptosis of NSCLC cells. Subsequently, the protein expression levels of target genes JAK2 and STAT3 after treatments with quercetin, curcumin, alpha-angelica lactone, and IL-6 were also detected by the Western blot analysis. We observed that the electrophoresis band width and band darkness of both phosphorylated JAK2 and STAT3 decreased conspicuously after treatments with quercetin, curcumin, and alpha-angelica lactone (represented by columns C, E, and G in Figure 13). This indicates lower expression of the JAK2 and STAT3 in comparison to the control group with only IL-6 treatment. Of all three ingredients, alpha-angelica lactone showcased the lowest inhibitory effect on both the expression of JAK2 and STAT3 proteins. Then, following the addition of JAK2 inhibitors on quercetin, there was another significant reduction in both JAK2 and STAT3 protein expression (represented by columns D and H). This indicates that JAK2 is upstream of STAT3 within the signaling pathway as the signaling cascade can't proceed with the repression of JAK2. The addition of STAT3 inhibitors to alpha-angelica lactone yielded a significant decrease in only the expression of STAT3, further proving the downstream position of STAT3. As JAK2 and STAT3 are both proteins that mediates cell proliferation, cell migration, and apoptosis, these results indicate that HDDGD ingredients may inhibit cell proliferation of NSCLC cells through IL-6/JAK2/STAT3.

DOI: 10.54254/2753-8818/15/20240482

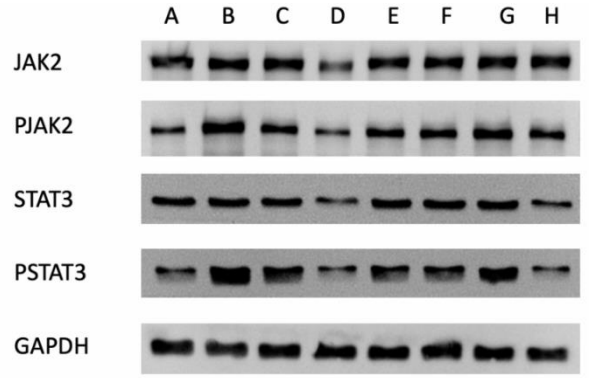

Figure 13. The protein expression levels of JAK2 and STAT3 after treatments with Quercetin, Curcumin, and Alpha-angelica lactone, measured by the Western Blot analysis. A represents the control, B represents IL-6 treatment, C represents Il-6 + Quercetin treatment, D represents IL-6 + Quercetin + JAK2 Inhibitor treatment, E represents IL-6 + Curcumin, F represents IL-6 + Curcumin + PI3K Inhibitor treatment, G represents IL-6 + Alpha-angelica lactone treatment, and H represents IL-6 + Alpha-angelica lactone + STAT3 Inhibitor treatment. PJAK2 represents phosphorylated JAK2 and PSTAT3 represents phosphorylated STAT3.

3.2.4. HQDGD inhibits cell migration of A549 cells. Cell migration is the fundamental process that underlies tumor-cell invasion and carcinogenesis. To investigate the effects of quercetin, curcumin, and alpha-angelica lactone on the cell migration of NSCLC cells, we conducted scratch assays after treating and incubating A549 cells for 24 hours (shown in figure 14). Cell migration was significantly inhibited after treatment with quercetin and curcumin compared to the negative and positive controls (individual treatments with IL-6), while the degree of cell migration remained similar after treatments with alpha-angelica lactone, indicating a weaker inhibitory effect. After the addition of JAK2 inhibitors to the A549 cells treated with quercetin, there was an elevated inhibition of cell migration, further supporting quercetin's function in repressing the signaling pathway of JAK2. However, there wasn't a prominent decrease in cell migration after the addition of PI3K inhibitors to curcumin and STAT3 inhibitors to alpha-angelica lactone.

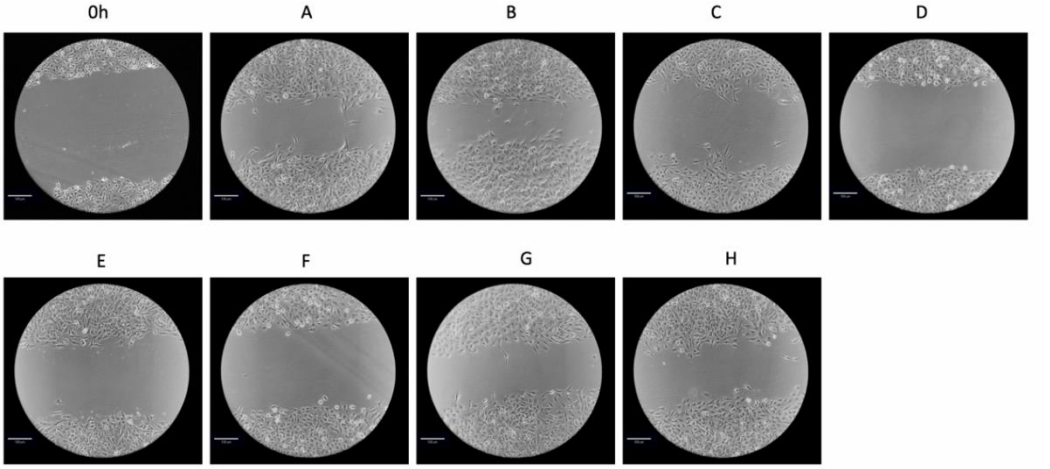

Figure 14. The degree of cell migration after 24-hour treatments with Quercetin, Curcumin, and Alpha-angelica lactone, measured by scratch assays. A represents the control, B represents IL-6 treatment, C represents Il-6 + Quercetin treatment, D represents IL-6 + Quercetin + JAK2 Inhibitor treatment, E represents IL-6 + Curcumin, F represents IL-6 + Curcumin + PI3K Inhibitor treatment, G represents IL-6 + Alpha-angelica lactone treatment, and H represents IL-6 + Alpha-angelica lactone + STAT3 Inhibitor treatment.

DOI: 10.54254/2753-8818/15/20240482

4. Discussion

This study investigated the effect of three HQDGD ingredients, curcumin, quercetin and alpha-angelica lactonee, on *IL6*, *JAK2*, *STAT3* and *PI3K*. Using Network Pharmacology and Experimental results triangulation, our investigation demonstrated the three chemicals' anti-proliferative and anti-migration properties on NSCLC. Each component decreases NSCLC's proliferative and migration properties, with a co-treatment of quercetin, alpha-angelica lactone and curcumin yielding the highest effect, suggesting the additive effects between the three chemicals. Furthermore, we also demonstrated the interference of curcumin on *JAK2* and *STAT3* phosphorylation, quercetin on *JAK2* phosphorylation and *IL6* expression, and alpha-Angelica lactone on *STAT3* expression.

Contemporary studies have demonstrated that quercetin interferes with the *IL6-JAK-STAT3* pathway by reducing the interleukin 6 (*IL6*) 's activation of downstream genes *GP130*, *JAK2* and *STAT3* [36]. Such inhibition resulted in a decrease in glioblastoma cells' migration potential [36]. Furthermore, quercetin was also found to interfere with cyclin D1 and matrix metalloproteinase-2 (*MMP-2*) 's gene expression, both of which are regulated by the *STAT3* gene, demonstrating the drug's potency to interfere with *IL6-JAK2-STAT3* pathway [36].

On the other hand, studies have found that curcumin inhibits Signal transducer and activator of transcription 3 (*STAT3*) phosphorylation and, as a result, downregulates the proliferative ability of NSCLC [37]. Other research has shown that applying curcumin to NSCLC suppresses *STAT3* phosphorylation, inhibiting colony formation and the cancer cell's ability to invade and migrate [37].

Other studies have also shown that alpha-angelica lactone contributes to *A.sinensis* extracts, including the active compound of alpha-angelica lactone, inhibits the *JAK2/STAT* and promotes apoptosis in breast cancer cells. However, the exact mechanism must be uncovered ("Angelica sinensis").

Upon research, our team found Wang et al.'s study has suggested a pathway of curcumin targets that yield significant anti-proliferative and anti-metastatic properties on NSCLC. Through laboratory experiments, Wang et al. [38] identified curcumin's suppressive effect on the *PI3K/AKT/mTOR* signalling pathway, offering yet another explanation of curcumin's impact on NSCLC. It is shown that PI3K activation leads to phosphatidylinositol (3,4,5)-trisphosphate (PIP3) production, which then activates Rho-guanine nucleotide exchange factors (GEF), inducing cell migration [39].

Interestingly, our team identified that curcumin has interfered with the *IL6- JAK2- STAT3* pathway not only by inhibiting *STAT3* but also by *JAK2* phosphorylation, which, to our knowledge, wasn't identified in earlier studies. Moreover, our experiment found that alpha-angelica lactone has an inhibitory effect on both *STAT3* and *JAK2* (although the inhibitory of *JAK2* phosphorylation isn't as significant as curcumin), which is also yet to be documented. Both results open up more possibilities for the research of HQDGD concerning NSCLC.

Our study also demonstrated HQDGD's inhibitory effect on gene targets downstream to *STAT3*: *HIF1*, *HIF2*, *VEGF* and *EGFR*, all of which are genetic hallmarks of cancer. Both Hypoxia inducible factor-1 and 2 (coded by *HIF1*, *HIF2*) are involved in angiogenesis and apoptosis; Vascular endothelial growth factor (coded by *VEGF*) is a potent angiogenic factor, and Epidermal growth factor receptor (coded by *EGFR*) is a pro-migration and division gene target in lung cancer cells [40, 41, 42]. Our finding suggests that HQDGD's inhibition of the *IL6- JAK2- STAT3* pathway might not only be limited to NSCLC but also common to many other cancer types.

There are many limitations to our study. Firstly, due to HERB's limited data, our study might have excluded a number of HQDGD ingredients present in the first stage, which will significantly affect our research direction and the final choice of chemicals and pathways. Using multiple databases will give a more holistic result. Secondly, we have used the Swiss Target Prediction tool to estimate the chemical's affinity to gene targets if no experimental results can be found in databases. However, to our knowledge, there are no experimental results that support the data given by the Swiss Target Prediction tool. Hence, although the chemical may have a high affinity to the gene target, it might not bind in vitro. Furthermore, due to ethical considerations, our experiments were conducted on cell lines instead of whole organisms. The inhibitory effect of curcumin, quercetin and alpha-angelica lactone on *IL6*-induced *STAT3/JAK2* pathway *in vivo* still needs to be tested.

DOI: 10.54254/2753-8818/15/20240482

5. Conclusion

In our work, we explored the treatment potential of Huangqi Danggui decoction, a traditional Chinese medicine, on non-small-cell lung cancer. The pivotal active ingredients of HQDGD, quercetin, curcumin, and alpha-angelica lactone, were successfully screened by conducting network pharmacology analysis on the protein-gene-pathway-target interactions. Simultaneously, the HQDBD and NSCLC common target genes were also obtained, namely *IL6*, *JAK2*, *STAT3* and *PI3K*. The inhibitory effects of the three active ingredients on NSCLC were then validated by drug-treating different combinations of them on A549 model cells. The gene and protein expression levels were also measured by quantitative PCR and Western blot analyses. Our results suggest that quercetin, curcumin, and alpha-angelica lactone expressed significant inhibitory effects on A549 cell proliferation and migration. Concurrently, we established that the *IL-6/JAK/STAT3* signaling pathway, which is critical to cell growth and apoptosis, is also downregulated by the above three ingredients. More investigations are required to uncover the molecular mechanisms of cell signaling pathway inhibitions and how it contributes to NSCLC carcinogenesis. Overall, we demonstrated the high therapeutic potential of HQDGD in inhibiting the cell proliferation and migration of NSCLC tumor cells.

Acknowledgement

This project was inspired by a school-organised visit to a local biotechnology company that quantifies and detects active ingredients in traditional herbal medicine. It was intriguing to observe the shift from using whole herbal ingredients to extracted compounds. We thank Mr. Varty for advising on the experimental design and gene targets.

References

[1] Sung, H., Ferlay, J., Siegel, R. L., Laversanne, M., Soerjomataram, I., Jemal, A., & Bray, F. (2021). Global cancer statistics 2020: Globocan estimates of incidence and mortality worldwide for 36 cancers in 185 countries. CA: A Cancer Journal for Clinicians, 71(3), 209–249. https://doi.org/10.3322/caac.21660

[2] Otano, I., Ucero, A. C., Zugazagoitia, J., & Paz-Ares, L. (2023). At the crossroads of immunotherapy for oncogene-addicted subsets of NSCLC. Nature Reviews Clinical Oncology, 20(3), 143–159. https://doi.org/10.1038/s41571-022-00718-x

[3] Chang, A. (2011). Chemotherapy, chemoresistance and the changing treatment landscape for NSCLC. Lung Cancer, 71(1), 3–10. https://doi.org/10.1016/j.lungcan.2010.08.022

[4] Current therapeutic strategies and challenges in NSCLC treatment: A comprehensive review. (2022). Experimental Oncology, 44(1). https://doi.org/10.32471/exp-oncology.2312-8852.vol-44-no-1.17411

[5] Kumar, M., & Sarkar, A. (2022). Current therapeutic strategies and challenges in NSCLC treatment: A comprehensive review. Experimental Oncology, 44(1). https://doi.org/10.32471/exp-oncology.2312-8852.vol-44-no-1.17411

[6] Rotow, J., & Bivona, T. G. (2017). Understanding and targeting resistance mechanisms in NSCLC. Nature Reviews Cancer, 17(11), 637–658. https://doi.org/10.1038/nrc.2017.84

[7] Ma, Y., Chen, M., Guo, Y., Liu, J., Chen, W., Guan, M., Wang, Y., Zhao, X., Wang, X., Li, H., Meng, L., Wen, Y., & Wang, Y. (2019). Prevention and treatment of infectious diseases by traditional Chinese medicine: A commentary. APMIS, 127(5), 372–384. https://doi.org/10.1111/apm.12928

[8] Chao, J., Dai, Y., Verpoorte, R., Lam, W., Cheng, Y.-C., Pao, L.-H., Zhang, W., & Chen, S. (2017). Major achievements of evidence-based traditional Chinese medicine in treating major diseases. Biochemical Pharmacology, 139, 94–104. https://doi.org/10.1016/j.bcp.2017.06.123

[9] The art and science of traditional medicine part 1: TCM Today — a case for integration. (2014). Science, 346(6216), 1569–1569. https://doi.org/10.1126/science.346.6216.1569-d

[10] Kong, D.-X., Li, X.-J., & Zhang, H.-Y. (2009). Where is the hope for drug discovery? let history tell the future. Drug Discovery Today, 14(3–4), 115–119. https://doi.org/10.1016/j.drudis.2008.07.002

[11] Ma, C., Jiang, Y., Wang, Y., & Xu, R. (2022). The latest research advances of Danggui Buxue Tang as an effective prescription for various diseases: A comprehensive review. Current Medical Science, 42(5), 913–924. https://doi.org/10.1007/s11596-022-2642-0

[12] Gao, Q. T., Choi, R. C. Y., Cheung, A. W. H., Zhu, J. T. T., Li, J., Chu, G. K. Y., Duan, R., Cheung, J. K. H., Jiang, Z. Y., Dong, X. B., Zhao, K. J., Dong, T. T. X., & Tsim, K. W. K. (2006). Danggui Buxue Tang - a Chinese herbal decoction activates the phosphorylations of extracellular signal-regulated kinase and estrogen receptorαin cultured MCF-7 cells. FEBS Letters, 581(2), 233–240. https://doi.org/10.1016/j.febslet.2006.12.018

[13] Wang, P., & Liang, Y.-Z. (2010). Chemical composition and inhibitory effect on hepatic fibrosis of Danggui Buxue decoction. Fitoterapia, 81(7), 793–798. https://doi.org/10.1016/j.fitote.2010.04.007

[14] Sun, X., Xu, X., Chen, Y., Guan, R., Cheng, T., Wang, Y., Jin, R., Song, M., & Hang, T. (2019). Danggui Buxue decoction sensitizes the response of non-small-cell lung cancer to gemcitabine via regulating deoxycytidine kinase and P-glycoprotein. Molecules, 24(10), 2011. https://doi.org/10.3390/molecules24102011

[15] Du, Q., Yang, K., & Sun, X. (2009). Efficacy of auxiliary therapy with Danggui Buxue Decoction No.1 in treating patients of non-small cell lung cancer at peri-operational stage. Chinese Journal of Integrative Medicine, 15(3), 184–188. https://doi.org/10.1007/s11655-009-0184-y

[16] Yu, B., Lv, G., Sohail, M., Li, Z., Li, Y., Yu, M., Sun, F., & Xu, H. (2022). Utilizing bioinformatics technology to explore the potential mechanism of Danggui Buxue decoction against NSCLC. Disease Markers, 2022, 1–20. https://doi.org/10.1155/2022/5296830

[17] Liu, Z., Guo, F., Wang, Y., Li, C., Zhang, X., Li, H., Diao, L., Gu, J., Wang, W., Li, D., & He, F. (2016). Batman-TCM: A bioinformatics analysis tool for molecular mechanism of traditional Chinese medicine. Scientific Reports, 6(1). https://doi.org/10.1038/srep21146

[18] Huang, L., Xie, D., Yu, Y., Liu, H., Shi, Y., Shi, T., & Wen, C. (2017). TCMID 2.0: A comprehensive resource for TCM. Nucleic Acids Research, 46(D1). https://doi.org/10.1093/nar/gkx1028

[19] "Herb." HERB, herb.ac.cn/.

[20] Olivier Michielin and Vicent Zoete. SwissADME, www.swissadme.ch/.

[21] Antoine Daina and others, SwissTargetPrediction: updated data and new features for efficient prediction of protein targets of small molecules, Nucleic Acids Research, Volume 47, Issue W1, 02 July 2019, Pages W357–W364, https://doi.org/10.1093/nar/gkz382

[22] Davies M, Nowotka M, Papadatos G, Dedman N, Gaulton A, Atkinson F, Bellis L, Overington JP. — Nucleic Acids Res. 2015; 43(W1):W612-20. doi: 10.1093/nar/gkv352

[23] "UniProt: the universal protein knowledgebase in 2023." Nucleic Acids Research 51, no. D1 (2023): D523-D531.

[24] Stelzer, G., Rosen, N., Plaschkes, I., Zimmerman, S., Twik, M., Fishilevich, S., ... & Lancet, D. (2016). The GeneCards suite: from gene data mining to disease genome sequence analyses. Current protocols in bioinformatics, 54(1), 1-30.

[25] Janet Piñero, Juan Manuel Ramírez-Anguita, Josep Saüch-Pitarch, Francesco Ronzano, Emilio Centeno, Ferran Sanz, Laura I Furlong. The DisGeNET knowledge platform for disease genomics: 2019 update. Nucl. Acids Res. (2019) doi:10.1093/nar/gkz1021

[26] Philippe Bardou, Jérôme Mariette, Frédéric Escudié, Christophe Djemiel and Christophe Klopp. jvenn: an interactive Venn diagram viewer. BMC Bioinformatics 2014, 15:293 doi:10.1186/1471-2105-15-293

[27] Szklarczyk, D., Kirsch, R., Koutrouli, M., Nastou, K., Mehryary, F., Hachilif, R., ... & von Mering, C. (2023). The STRING database in 2023: protein–protein association networks and functional

enrichment analyses for any sequenced genome of interest. Nucleic acids research, 51(D1), D638-D646.

[28] Shannon P., Markiel A., Ozier O., Baliga N. S., Wang J. T., Ramage D., et al. (2003). Cytoscape: a software environment for integrated models of biomolecular interaction networks. Genome Res. 13 2498–2504. 10.1101/gr.1239303

[29] Tang, Yu et al. “CytoNCA: a cytoscape plugin for centrality analysis and evaluation of protein interaction networks.” Bio Systems vol. 127 (2015): 67-72. doi:10.1016/j.biosystems. 2014.11.005

[30] Ashburner, M., Ball, C. A., Blake, J. A., Botstein, D., Butler, H., Cherry, J. M., ... & Sherlock, G. (2000). Gene ontology: tool for the unification of biology. Nature genetics, 25(1), 25-29.

[31] Aleksander, S. A., Balhoff, J., Carbon, S., Cherry, J. M., Drabkin, H. J., Ebert, D., ... & Zarowiecki, M. (2023). The Gene Ontology knowledgebase in 2023. Genetics, 224(1), iyad031.

[32] Kanehisa, M., & Goto, S. (2000). KEGG: kyoto encyclopedia of genes and genomes. Nucleic acids research, 28(1), 27-30.

[33] Kanehisa, M. (2019). Toward understanding the origin and evolution of cellular organisms. Protein Science, 28(11), 1947-1951.

[34] Kanehisa, M., Furumichi, M., Sato, Y., Kawashima, M., & Ishiguro-Watanabe, M. (2023). KEGG for taxonomy-based analysis of pathways and genomes. Nucleic acids research, 51(D1), D587-D592.

[35] B.T. Sherman, M. Hao, J. Qiu, X. Jiao, M.W. Baseler, H.C. Lane, T. Imamichi and W. Chang. DAVID: a web server for functional enrichment analysis and functional annotation of gene lists (2021 update). Nucleic Acids Research. 23 March 2022. 50(W1):W216-W221. doi:10.1093/nar/gkac194.[PubMed].

[36] Michaud-Levesque, Jonathan, et al. "Quercetin Abrogates IL-6/STAT3 Signaling and Inhibits Glioblastoma Cell Line Growth and Migration." Experimental Cell Research, vol. 318, no. 8, May 2012, pp. 925-35. Pubmed, https://doi.org/10.1016/j.yexcr.2012.02.017.

[37] Wan Mohd Tajuddin, Wan Nur Baitty, et al. "Mechanistic Understanding of Curcumin’s Therapeutic Effects in Lung Cancer." Nutrients, vol. 11, no. 12, 6 Dec. 2019, p. 2989. Pubmed, https://doi.org/10.3390/nu11122989.

[38] Wang, Naizhi, et al. "Curcumin Inhibits Migration and Invasion of Non-small Cell Lung Cancer Cells through Up-regulation of MiR-206 and Suppression of PI3K/AKT/mTOR Signaling Pathway." Acta Pharmaceutica, vol. 70, no. 3, 17 Feb. 2020, pp. 399-409. Pubmed, https://doi.org/10.2478/acph-2020-0029.

[39] Millar, Fraser R., et al. "Epithelial Cell Migration as a Potential Therapeutic Target in Early Lung Cancer." European Respiratory Review, vol. 26, no. 143, 31 Jan. 2017, p. 160069. Nature, https://doi.org/10.1183/16000617.0069-2016.

[40] Uribe, Mary Luz et al. "EGFR in Cancer: Signaling Mechanisms, Drugs, and Acquired Resistance." Cancers vol. 13,11 2748. 1 Jun. 2021, doi:10.3390/cancers13112748

[41] Zhao, J., Du, F., Shen, G. et al. The role of hypoxia-inducible factor-2 in digestive system cancers. Cell Death Dis 6, e1600 (2015). https://doi.org/10.1038/cddis.2014.565

[42] Duffy AM, Bouchier-Hayes DJ, Harmey JH. Vascular Endothelial Growth Factor (VEGF) and Its Role in Non-Endothelial Cells: Autocrine Signalling by VEGF. In: Madame Curie Bioscience Database [Internet]. Austin (TX): Landes Bioscience; 2000-2013. Available from: https://www.ncbi.nlm.nih.gov/books/NBK6482/